ASSESSING THE IMPACTS OF LAND USE AND LAND COVER CHANGES ON LAND SURFACE TEMPERATURE IN RAPIDLY URBANIZING ENVIRONMENTS: A CASE STUDY OF RAJSHAHI CITY, BANGLADESH

Aabeer Kumar Saha Aakash[*1], Suchi Nandi Puja[2]

[1] *Student, Department of Water Resources Engineering, Bangladesh University of Engineering and Technology, Bangladesh, e-mail: aabeeraakashcc@gmail.com*
[2] *Student, Department of Water Resources Engineering, Bangladesh University of Engineering and Technology, Bangladesh, e-mail: suchipuja30@gmail.com*

*Corresponding Author

ABSTRACT

Land use and land cover (LULC) changes profoundly affect environmental dynamics, with urbanization representing a global concern due to its transformative influence on natural landscapes. This study presents a comprehensive analysis of land use and land cover (LULC) change patterns and their intricate relationship with land surface temperature (LST) within the Rajshahi City Corporation (RCC) areas over the past three decades. Utilizing Landsat TM/OLI satellite imagery for the years 1993, 2003, 2013, and 2023, LULC effects on LST were investigated, encompassing LST distribution across diverse land use categories, LULC-wise LST variations, and correlations between land use indices (NDVI, NDBI, NDBaI, and NDWI) and LST. The study period saw a 222.88% increase in built-up areas (7.43% per year) and a decrease in vegetation and agricultural lands by 49.55% (1.65% per year). Bare lands increased by 39.24% (1.31% per year), while water bodies increased negligibly by 12.48% (0.42% per year). Built-up areas gradually increased over the study period, while bare soil saw a sudden increase in the final stage (2013-2023) and is expected to be converted to built-up areas in the near future. From 1993 to 2003, 2003-2013, and 2013-2023, built-up areas gained 9.30%, 6.71%, and 11.94%, respectively, from vegetative and agricultural lands, highlighting the rapid progress of urbanization, consistently converting vegetative and agricultural lands to built-up areas, followed by bare lands and water bodies. The expansion of urban regions altered the radiative properties of the surface, causing an imbalance in the energy budget. This, in turn, led to an increasing trend in LST of 0.57°C per year between 1993 and 2003. The spatial distribution of LST in Rajshahi City Corporation showed that 74% of the area had temperatures ranging from 32 to 36 °C, with some extreme temperature zones of 36 to 40 °C due to compact urbanization. Furthermore, the study reveals that the city's LST is increasing at an alarming rate with time. The mean LST gradually increased from 1993 to 2023, irrespective of land cover type. Built-up areas and bare soil showed a higher LST, while water bodies and vegetative and agricultural lands showed the lowest LST. Correlation analysis shows a negative relationship between NDVI and NDWI with LST, highlighting the cooling effect of vegetation and water, while NDBI and NDBaI exhibit a positive correlation with LST. These results provide vital insights for urban planners and environmental engineers, aiding their understanding of the impacts of LULC changes on LST and offering a basis for informed policy measures to mitigate the adverse effects of rapid urban growth.

Keywords: *Land use and land cover (LULC) change, Land Surface Temperature (LST), Landsat, NDVI, Rajshahi City Corporation (RCC)*

1. INTRODUCTION

Urbanization is reshaping cities worldwide, and Rajshahi City in Bangladesh is a compelling case study revealing variations in land surface temperature (LST) resulting from urban expansion. It is imperative to comprehend the intricate correlation between land use and land cover (LULC) changes and the dynamics of LST within the Rajshahi City Corporation (RCC). As the city's population has exceeded 800,000, with a significant urbanization rate of 32.93% (Kanti Jodder et al., 2020), it threatens the city's environmental sustainability. Projections have shown that more than sixty percent of the city will become an urban settlement by 2040 (Rouf, 2018). The situation is distinct in Rajshahi City, primarily driven by unplanned urbanization and significant population movement (Das & Haque, 2022). Climate-induced forced migration further complicates the urban landscape caused by food insecurity and floods, leading to population displacement (Rahman et al., 2022). Following relocation, numerous migrants reside in urban slums, facing poor-paying jobs and lacking access to essential services such as water (Ahsan et al., 2014).

One crucial environmental indicator susceptible to LULC changes is LST. LST experiences significant fluctuations during urbanization, especially in rapidly growing areas like Rajshahi. In urban and environmental research, GIS and Remote Sensing have proven invaluable for investigating the impacts of LULC changes on LST (Dewan & Corner, 2013). Although extensive research has been conducted on the relationship between LULC changes and LST in various international cities, such studies are rare in the case of Rajshahi (RDA, 2008). Kafy et al. (2020a) and Dey et al. (2021) both found that the expansion of built-up areas and reduction of green spaces has led to a rise in land surface temperature, with Kafy (2020b) predicting a further increase in temperature if current urban growth trends continue. This study contributes to filling the research gap by investigating the impacts of LULC modifications on LST within the RCC and correlations between LST and land cover indices, such as NDVI, NDWI, NDBI, and NDBaI. This research supports previous studies and provides valuable insights for urban planners and environmental engineers to comprehend the impact of LULC modifications on LST, which can aid in the development of policies.

2. METHODOLOGY

2.1 Study Area

The Rajshahi City Corporation (RCC), under the supervision of the Ministry of Local Government, holds substantial significance within the administrative framework of Bangladesh. It goes back to when the Rajshahi Municipality was started in 1876 and transformed into Rajshahi Municipal Corporation in 1987. Presently, it is recognized as the RCC. Geographically located on the Padma River, situated between latitudes 24°20'-24°24' north and longitudes 88°32'-88°40' east (Figure 1), the RCC is positioned in a fertile region that is renowned for its cultural heritage and abundant agricultural resources, particularly rice and mango cultivation (BBS, 2013). During the months of April and May, the RCC experiences temperature variations ranging from 10°–27° degrees to 24°–40° degrees. The Bangladesh Meteorological Department (BMD) designates the RCC as falling within the western dry zone, receiving an annual average precipitation of 1419 mm. The precipitation is characterized by distinct seasonal transitions, including Winter (mid-December to February), Pre-monsoon (March to May), Monsoon (June to mid-October), and Post-monsoon (mid-October to December) showcasing reduced rainfall and temperatures (Clemett et al., 2006).

With a population exceeding half a million and a density of 9370 per km² (BBS, 2013), the RCC has observed rapid urbanization, resulting in a decline of more than 30% in vegetation coverage over the past five decades, consequently leading to an increase in land surface temperatures (Kafy et al., 2020b). The intricate transformation of the RCC's landscape serves as evidence of its complexity, thereby motivating our study to investigate the interconnections between urbanization, changes in

land use, and the subsequent rise in land surface temperatures within this dynamic system (Clemett et al., 2006).
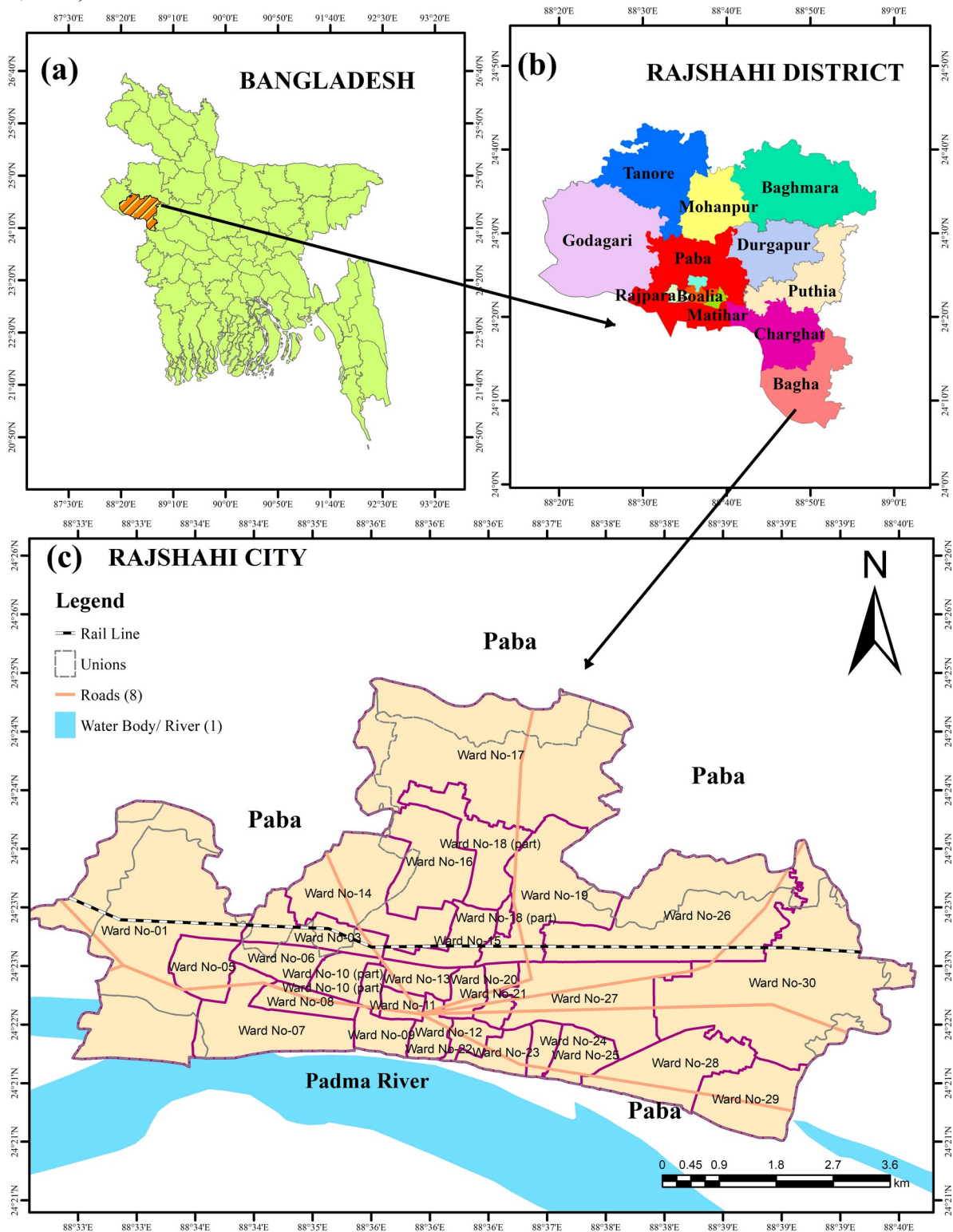
Figure 1: Location of (a) Rajshahi district in Bangladesh, (b) Rajshahi City Corporation in Rajshahi district, and (c) Detailed administrative map of the study area.

2.2 Data Collection and Image Processing

The study examined LULC and LST changes in Rajshahi City Corporations using remotely sensed data of four datasets from the Multispectral Landsat satellite series between 1993 and 2023. The US

Geological Survey provided satellite images with less than 10% cloud cover taken in January to minimize seasonal effects. The acquired Landsat data were rigorously pre-processed, emerging as pre-georeferenced level 1 terrain (L1T) corrected products that underwent rigorous geometric and radiometric calibration. Additionally, the USGS completed resampling operations and produced thermal bands for all Landsat scenes at a resolution of up to 30 meters, harmonizing them with the sensor multispectral bands (NASA, 2010). Table 1 contains essential information such as acquisition date, sensor specifics, path/row identification, and cloud cover percentage.

Table 1: Information on Landsat satellite images

Acquisition Date	Satellite/Sensor	Path/Row	Cloud Cover (%)
22 January, 1993	Landsat 5 (TM)	138/43	0.00
26 January, 2003	Landsat 7 (ETM+)	138/43	2.00
21 January, 2013	Landsat 7 (ETM+)	138/43	0.00
25 January, 2023	Landsat 9 (OLI-2/TIRS-2)	138/43	0.00

2.3   Land Cover Classification

The study utilized the Maximum Likelihood Supervised Classification (MLSC) method to identify distinct LULC classes from Landsat images. The four primary LULC classes were water bodies, built-up areas, vegetation and agricultural lands, and bare lands. The selection of the primary land cover classes was guided by earlier studies (Kafy et al., 2020a), with Table 2 providing additional details for each of the four primary land cover classes. To aid in the classification process, composite band images were used to collect 500 signatures, which were merged and analysed using the MLSC technique. The RGB colour compositions 432 and 321 were chosen for natural colour representation for Landsat 5/7 and Landsat 8/9, respectively, while 543 and 432 were selected for colour infrared (CIR) composition. The MLSC technique was applied to classify all cells in the output raster, with each class being assigned an equal probability weight attached to their respective signatures (Imran et al., 2021) and excluding any object found on the image that was deemed too small, covering fewer than three pixels (Tanjina Hasnat, 2022).

Table 2: Land cover classes and corresponding land use types

Classes	Description
Waterbody	Wetlands, gullies, marshy areas, low-lying lands, and gullies.
Built-up Area	Residential areas, industrial zones, commercial sectors, settlements, roads, mixed urban regions, and impervious surfaces like pavements.
Vegetation and Agricultural Lands	Open spaces, landfill sites, brickfields, barren soil, construction areas, abandoned lands, and uncultivated grounds.
Bare Lands	Crop fields, fruit orchards, cultivated lands, fallow areas, forests, trees, vegetated lands, mixed forested areas, and gardens.

2.4 Land Surface Temperature (LST) Computation

LST is a crucial parameter for understanding the Earth's surface behaviour and interaction with its surroundings. Thermal sensors on several satellite platforms, such as Landsat 5 TM, Landsat 7 ETM+, and Landsat 9 OLI-2/TIRS-2, are used to measure LST of various terrains, including soil, water bodies, vegetation, and built-up areas. However, analysing LST using satellite thermal data requires a comprehensive process, including sensor radiometric alignment, air and surface reflectance correction, and accounting for spatial variations in LULC. The Mono Window Algorithm (MWA) was employed in this study for efficient LST retrieval, as it provides a simple and effective approach. The MWA technique depends on three primary parameters, ground emissivity, atmospheric transmittance, and effective mean atmospheric temperature, to derive LST from a single Landsat band (Ding & Shi, 2013).

To calculate LST from Landsat 9 OLI-2/TIRS-2, six steps were applied, whereas from Landsat 5 TM and Landsat 7 ETM+, only the first two steps were needed:

Step 1: Conversion of Digital Number (DN) to Spectral Radiance (L_λ)
Solar energy collected by sensors such as Landsat 5 (TM), Landsat 7 (ETM+), and Landsat 9 (OLI-2/TIRS-2) is transformed into Top of Atmosphere (ToA) spectral radiance through the utilization of manual equations, specifically equation (1a) for Landsat 5 (TM) and Landsat 7 (ETM+), and equation (1b) for Landsat 9 (OLI-2/TIRS-2).

$$L_\lambda = \frac{L_{max} - L_{min}}{Q_{calmax} - Q_{calmin}} \times \left(Q_{cal} - Q_{calmin} \right) + L_{min} \qquad (1a)$$

Where, L_λ is the spectral radiance in (Watts/(m²×sr×μm)), L_{max} and L_{min} are the maximum and minimum spectral radiance of the sensor, which is scaled to Q_{calmax} in (Watts/(m²×sr×μm)) and Q_{calmin} in (Watts/(m²×sr×μm)) respectively and Q_{cal} is the quantized calibrated pixel value.

$$L_\lambda = M_L \times Q_{cal} + A_L - O_i \qquad (1b)$$

Where, L_λ is the Top of Atmosphere (ToA) spectral radiance in (Watts/(m²×sr×μm)), M_L and A_L are the band-specific multiplicative and additive rescaling factor, and O_i is the correction value.

Step 2: Conversion of Spectral Radiance (L_λ) to Brightness Temperature (BT)

$$BT = \frac{K_2}{\ln\left(\frac{K_1}{L_\lambda} + 1\right)} - 273.15 \qquad (2)$$

Where, BT is the brightness temperature in (°C), and K_1 and K_2 are the band-specific thermal conversion constants from the metadata.

Step 3: NDVI Method for Emissivity Correction

$$NDVI = \frac{NIR - R}{NIR + R} \qquad (3)$$

Where, NDVI is the Normalized Difference Vegetation Index, NIR is the near-infrared band, and R is the red band.

Step 4: Calculating the Proportion of Vegetation (P_v)

$$P_v = \frac{NDVI - NDVI_{min}}{NDVI_{max} - NDVI_{min}}^2 \qquad (4)$$

Where, P_v is the Proportion of Vegetation, $NDVI_{min}$ and $NDVI_{max}$ are the minimum and maximum NDVI values respectively from NDVI image.

Step 5: Calculating Land Surface Emissivity (LSE)

$$\varepsilon = 0.004 \times P_v + 0.986 \qquad (5)$$

Where, ε is the LSE, 0.004 and 0.986 are correction values of the equation assigned to a particular correspondence.

Step 6: Calculating Land Surface Temperature (LST)

$$LST = \frac{BT}{1 + \frac{\lambda \times BT}{\rho} \ln(\varepsilon)} \qquad (6)$$

Where, LST is the Land Surface Temperature in (°C), λ is the wavelength of emitted radiance in meters, and ρ is calculated as:

$$\rho = h\frac{c}{\sigma} = 1.438 \times 10^{-2} \, mK \qquad (7)$$

Where, σ is the Boltzmann constant $\left(1.38 \times 10^{-23} J/K\right)$, h is Planck's constant $\left(6.626 \times 10^{-34} Js\right)$, and c is the velocity of light $\left(2.998 \times 10^8 m/s\right)$.

2.5 Land Use Indices Computation

The Normalized Difference Vegetation Index (NDVI), Normalized Difference Water Index (NDWI), Normalized Difference Built-up Index (NDBI), and Normalized Difference Built-up Area Index (NDBaI) are calculated using the equations (8), (9), (10), and (11):

$$NDVI = \frac{NIR - R}{NIR + R} \tag{8}$$

$$NDWI = \frac{G - NIR}{G + NIR} \tag{9}$$

$$NDBI = \frac{NIR - SWIR}{NIR + SWIR} \tag{10}$$

$$NDBaI = \frac{SWIR - TIR}{SWIR + TIR} \tag{11}$$

Where, NIR is the near-infrared band, R is the red band, G is the green band, SWIR is the shortwave infrared band, and TIR is the thermal infrared band.

3. RESULTS AND DISCUSSION

3.1 Analysis of Land Use Land Cover (LULC) Changes

The study generated a final classified map displaying the spatial distribution of various land cover in RCC for the years 1993, 2003, 2013, and 2023 (Figure 2). Additionally, Table 3 presents changes in percentage and mean change in percentage for the entire study period.
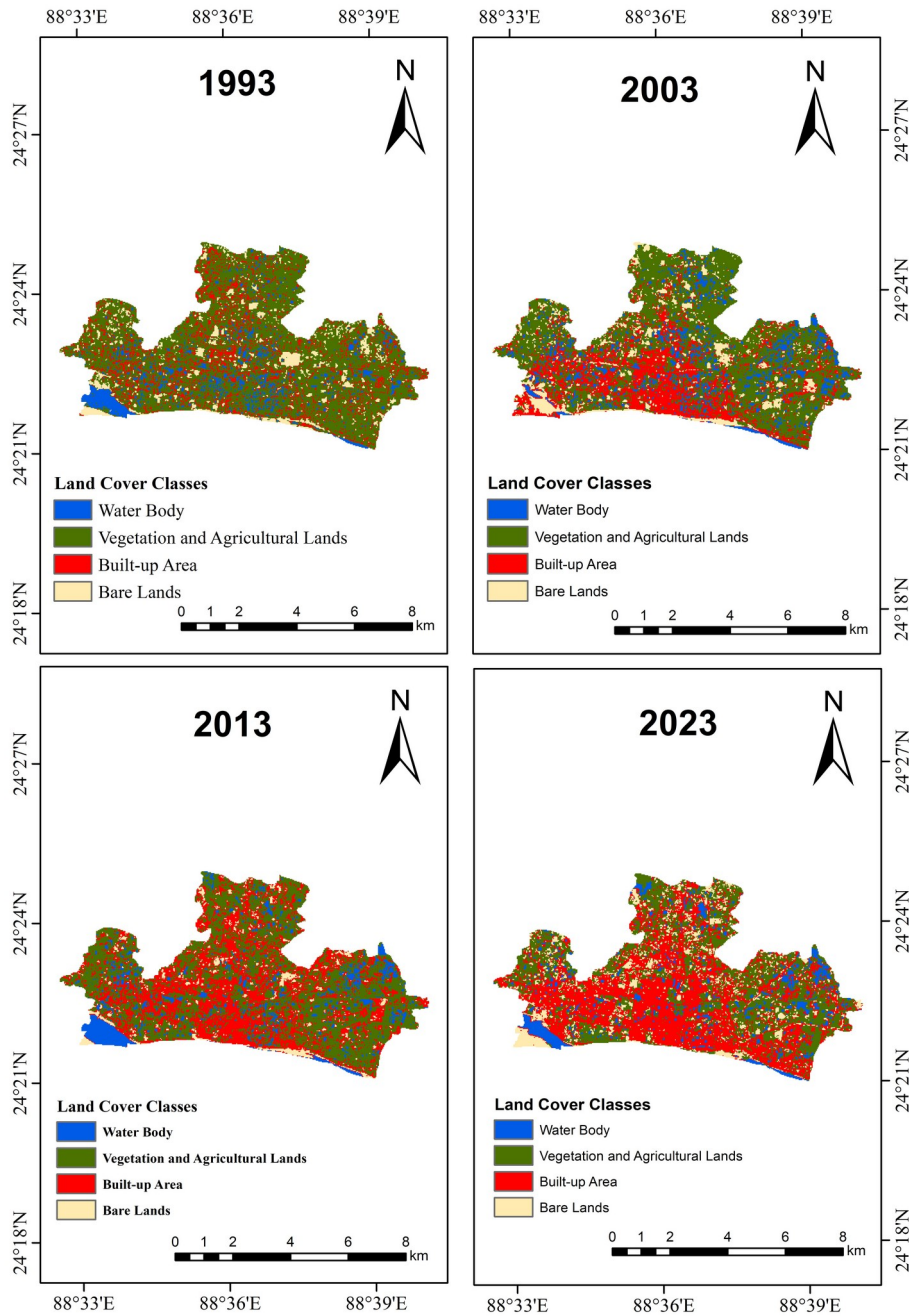
Figure 2: Land cover map of Rajshahi City Corporation for the years (a) 1993, (b) 2003, (c) 2013, and (d) 2023.

Over the study period from 1993 to 2023, the built-up area experienced a significant increase of 222.88% (7.43% annually), while vegetation and agricultural lands decreased by 49.55% (1.65% annually). On the other hand, the bare lands increased by 39.24% (1.31% annually), while the increase in water bodies was negligible (0.42% annually). The built-up area experienced a gradual increase throughout the study period, whereas bare soil increased abruptly in the final phase of the study period (2013–2023), which is expected to be converted into a built-up area in the near future. This was possible due to a significant decrease in vegetation and agricultural lands during the study period (Table 3).

A land cover change matrix analysis was conducted to evaluate the conversion of land cover classes from 1993 to 2023. The results revealed that 59.51%, 59.86%, and 54.14% of the study area remained unchanged during the periods 1993-2003, 2003-2013, and 2013-2023, respectively, while the remaining area underwent mutual conversion among the four land cover classes. Figure 3 displays the gains, losses, and net changes of the four land cover classes based on mutual conversion.

Table 3: Percentage of different land cover and its change in different periods

Land Cover Classes	1993 Area (%)	2003 Area (%)	2013 Area (%)	2023 Area (%)	1993-2003 Percentage Change (%)	1993-2003 Mean Change (% / year)	2003-2013 Percentage Change (%)	2003-2013 Mean Change (% / year)	2013-2023 Percentage Change (%)	2013-2023 Mean Change (% / year)	1993-2023 Percentage Change (%)	1993-2023 Mean Change (% / year)
Bare Lands	8.27	10.06	4.85	11.52	21.59	2.16	-51.76	-5.18	137.41	13.74	39.24	1.31
Built-up Area	13.82	24.52	35.08	44.63	77.34	7.73	43.10	4.31	27.23	2.72	222.88	7.43
Vegetation and Agricultural Lands	70.58	55.08	51.16	35.61	-21.95	-2.20	-7.13	-0.71	-30.41	-3.04	-49.55	-1.65
Waterbody	7.33	10.34	8.91	8.24	41.18	4.12	-13.86	-1.39	-7.51	-0.75	12.48	0.42
Total	100	100	100	100								

The study identified two prominent changes in land cover trends: a decline in vegetative and agricultural lands and an increase in built-up areas. To better understand this shift, we analyzed the contributions of other land cover classes to the net change in these areas, as depicted in Figure 4. From 1993-2003, 2003-2013, and 2013-2023, built-up areas gained 9.30%, 6.71%, and 11.94%, respectively, from vegetative and agricultural lands. The data highlights the rapid progress of urbanization, which consistently converts vegetative and agricultural lands to built-up areas, followed by bare lands and water bodies.
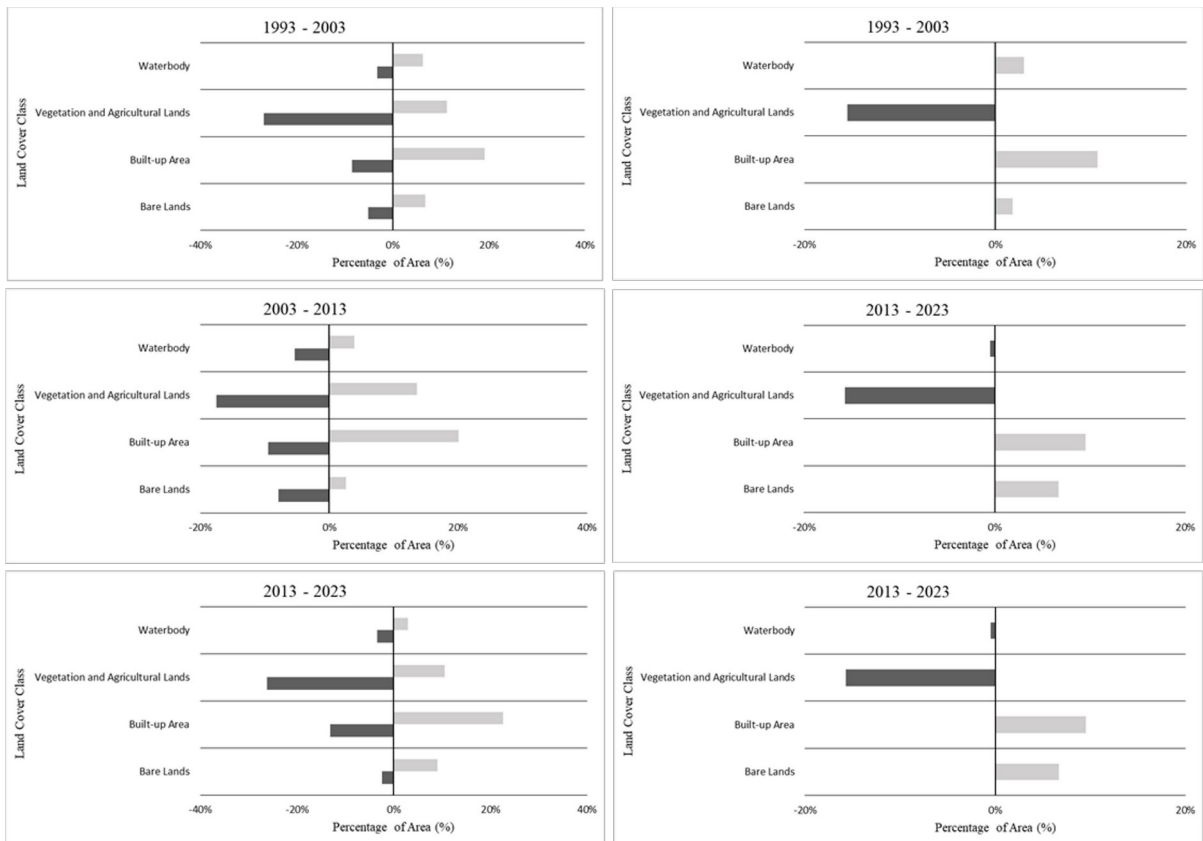
Figure 3: (a) Gains and losses, and (b) Net changes of the four land cover classes between 1993-2003, 2003-2013, and 2013-2023.
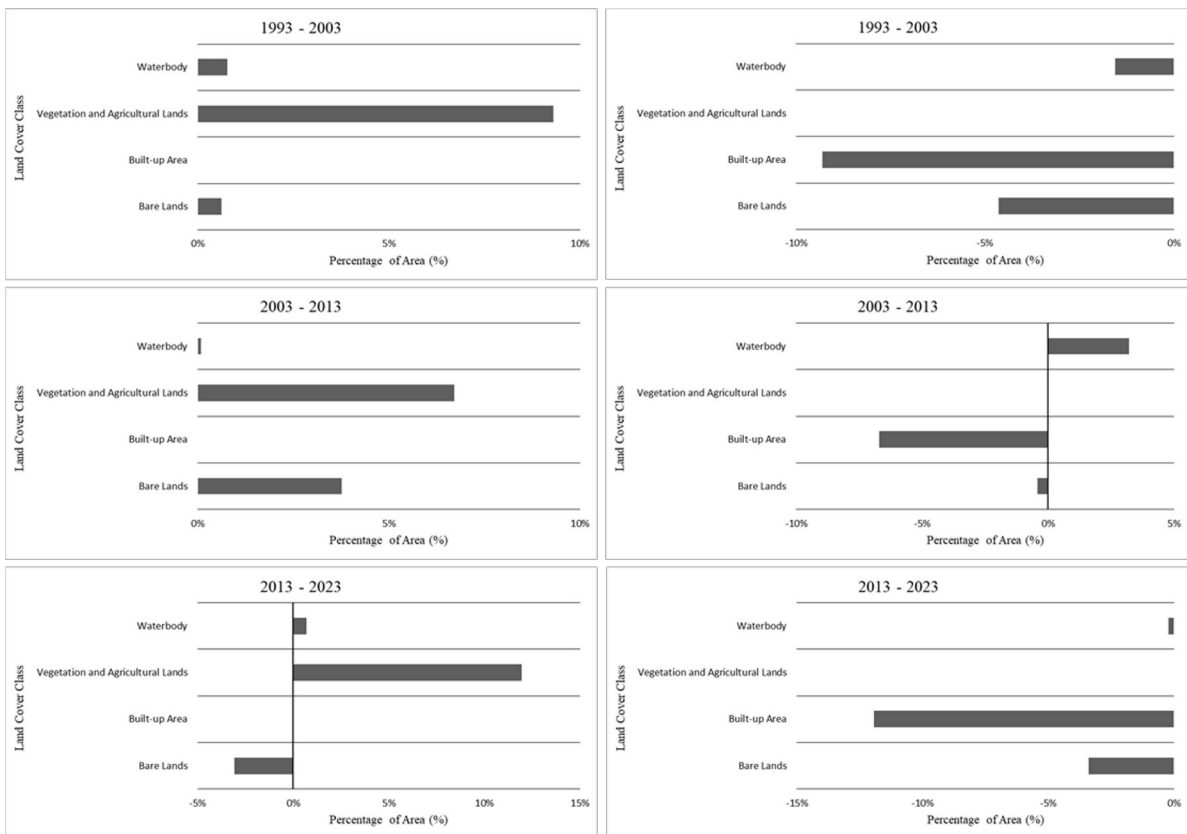
Figure 4: Contribution to net change in (a) Built-up area, and (b) Vegetation and agricultural lands in between 1993-2003, 2003-2013, and 2013-2023.

3.2 Analysis of Land Surface Temperature (LST) Changes

A study of the LST of RCC shows that it has undergone significant changes over time due to meteorological conditions and urbanization. The LSTs of 1993, 2003, 2013, and 2023 are presented in Table 4, while Figure 5 illustrates the classification of LSTs over the same period.
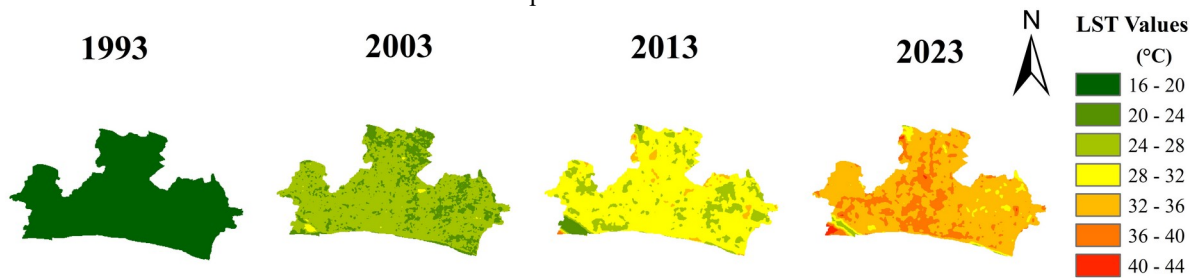
Figure 5: LST map of Rajshahi City Corporation for the years (a) 1993, (b) 2003, (c) 2013, and (d) 2023.

The mean temperature rose from 17.66 °C in 1993 to 28.98 °C in 2013, with temperature zones between 28 and 32 °C being the most widespread. By 2023, most areas (74%) had temperatures ranging from 32 to 36 °C (Figure 6), with some extreme temperature zones of 36 to 40 °C due to compact urbanization. The study found that the spatial mean increase of LST for the study area was 17.16 °C, at the rate of 0.57 °C per year from 1993 to 2003. In conclusion, the study reveals that the city's LST is increasing at an alarming rate with time.

Table 4: Land surface temperature in different years

Year	Minimum (°C)	Maximum (°C)	Mean (°C)	Standard Deviation
1993	16.10	20.18	17.66	0.50
2003	20.26	30.27	24.83	1.03
2013	21.82	37.25	28.98	1.68
2023	27.02	41.62	34.82	1.74

3.3 Variations of Land Surface Temperature for Different Land Covers

Table 5 shows the maximum, minimum, and mean LST values across land cover classes for 1993, 2003, 2013, and 2023. The mean LST increased for all land covers from 1993 to 2023, with the highest LST observed for bare lands, followed by built-up areas, vegetation and agricultural lands, and water bodies. This is similar to previous studies, considering we investigated the LST during winter. LST in different land cover might vary due to data acquisition time because built-up surfaces gain heat more slowly than bare soil. However, bare soil releases more heat quickly than built-up surfaces (Ogunjobi et al.,2018).
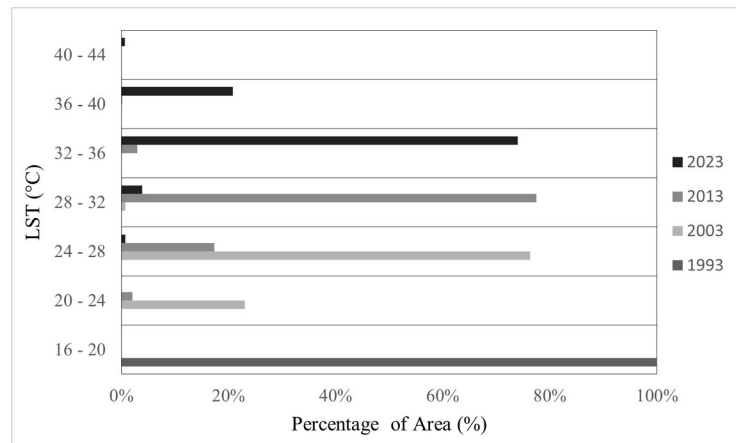
Figure 6: Distribution of area in various LST classes.

3.4 Variations of Land Surface Temperature for Different Land Covers

LST varies with land cover. To investigate the impact of LULC changes on LST, it is essential to use the thermal signature of each land cover. To establish the relationship between LST and LULC, four indices, NDVI, NDWI, NDBI, and NDBaI, were used (Figure 7). The lower the NDVI value, the higher the LST, as dense vegetation and trees induce more evapotranspiration, leading to lower temperature phenomena. The NDWI values decreased over the years, indicating that the LST increased in areas with lower NDWI and higher NDBaI. The NDBI value gradually increased, leading to higher LST values. The result of linear regression and multiple correlations indicates a strong and positive correlation between LST, NDBI, and NDBaI and a strongly negative correlation between LST, NDVI, and NDWI (Figure 8).

Table 5: Land surface temperature in different land use classes

Year	Bare Lands			Built-up Area			Vegetation and Agricultural Lands			Waterbody		
	Minimum (°C)	Maximum (°C)	Mean (°C)	Minimum (°C)	Maximum (°C)	Mean (°C)	Minimum (°C)	Maximum (°C)	Mean (°C)	Minimum (°C)	Maximum (°C)	Mean (°C)
1993	16.81	20.18	17.95	16.74	19.73	17.73	16.10	20.18	17.64	16.56	18.83	17.35
2003	22.84	30.27	25.90	22.33	28.82	25.30	22.33	29.31	24.63	20.26	26.86	23.79
2013	25.44	37.25	30.74	24.70	36.45	29.83	23.32	33.80	28.68	21.82	31.97	26.49
2023	31.16	41.62	35.70	29.35	41.09	35.60	27.66	40.13	34.11	27.02	40.83	32.47
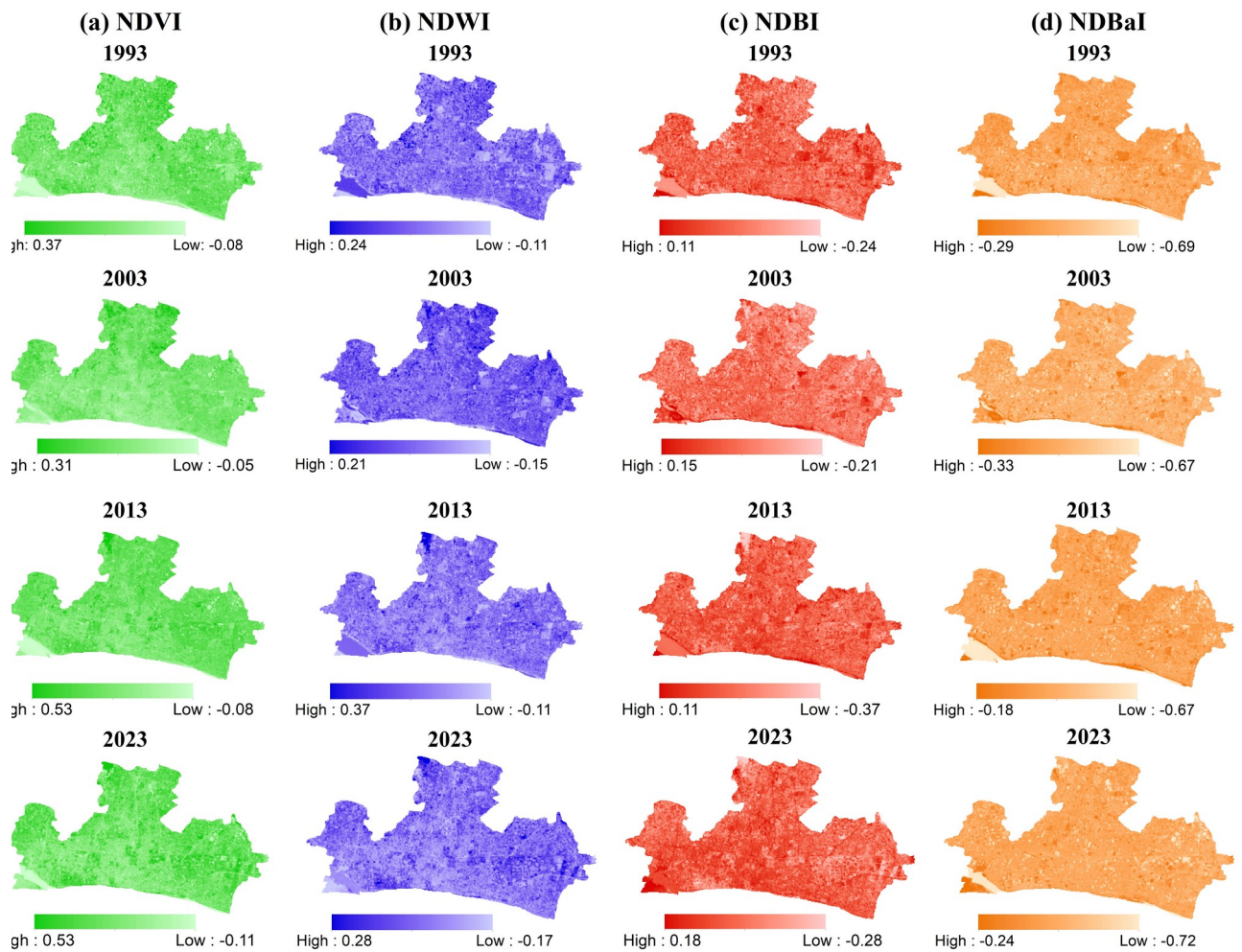
Figure 7: Spatial distribution map of (a) NDVI, (b) NDWI, (c) NDBI, and (d) NDBaI for the years 1993, 2003, 2013, and 2023.

4. CONCLUSIONS

In summary, our study underscores the concerning increase of LST within RCC due to rapid urbanization. The analysis highlights a significant transformation in land cover patterns, primarily driven by urban expansion and socioeconomic advancement. Over the study period, the built-up areas

surged by an alarming 222.88%, marking an annual growth of 7.43%, while vegetation and agricultural lands declined sharply by 49.55% (1.65% annually). The observed surge in built-up areas alongside the drastic reduction in vegetative and agricultural lands signifies the extensive impact of rapid urban expansion on the city's landscape. This expansion significantly altered the surface's radiative properties, causing an imbalance in the surface energy budget and a subsequent rise in LST, increasing at a rate of 0.57 °C per year from 1993 to 2003. The distribution of LST within Rajshahi City Corporation showcased approximately 74% of the area experiencing temperatures between 32 to 36 °C, with zones reaching extreme temperatures of 36 to 40 °C. The spatial distribution of LST reflects a concerning rise, especially in zones experiencing concentrated urbanization, portraying a clear trend of increasing temperatures over time.
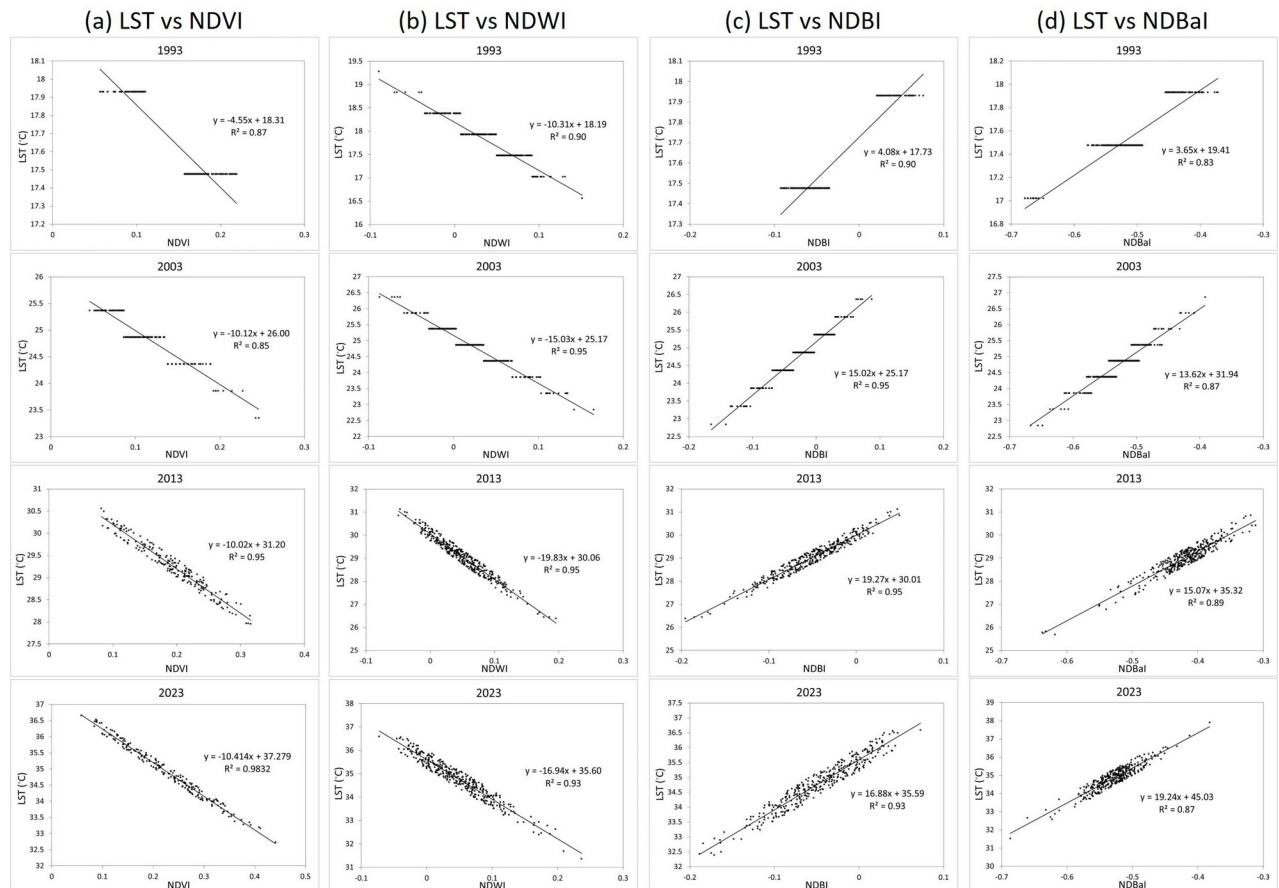
Figure 8: Spatial plot for (a) LST vs NDVI, (b) LST vs NDWI, (c) LST vs NDBI, and (d) LST vs NDBaI for the years 1993, 2003, 2013 and 2023.

The study's findings highlight an overall increase in mean LST from 1993 to 2023 across all land cover types, with built-up areas and bare soil having higher LST, while water bodies and vegetative and agricultural lands had the lowest LST. This increase primarily resulted from urbanization, signifying the urban heat island effect. The study's results revealed intricate relationships between land cover and LST, with a negative correlation between LST and NDVI and NDWI, and a positive correlation between LST and NDBI and NDBaI.

Our study underscores the urgency for environmental engineers, urban planners, and policymakers to address the implications of rising LST caused by urbanization. Formulating strategic interventions and growth management policies becomes imperative to mitigate the urban heat island effect and its associated challenges. Ultimately, this research aims to advance the discourse on urbanization's impact on land cover changes and LST, crucial in guiding sustainable urban development strategies worldwide.

ACKNOWLEDGEMENTS

REFERENCES

Ahsan, R., Kellett, J., & Karuppannan, S. (2014). Climate Induced Migration: Lessons from Bangladesh. The International Journal of Climate Change: Impacts and Responses, 5(2), 1–15.

(Bangladesh Bureau of Statistics), BBS. (2013). District statistics, Rajshahi. Ministry of Planning, Government of the People's Republic of Bangladesh. Bangladesh Bureau of Statistics.

Clemett, A. (2006). Background information for Rajshahi City, Bangladesh.

Das, A., & Haque, S. (2022). Promoting Circular Waterway Transport System for Recreational Water Environments and Integrated Urban Transportation Systems in Rajshahi City, Bangladesh.

Dewan, A. M., & Corner, R. J. (2013). Impact of Land Use and Land Cover Changes on Urban Land Surface Temperature. Dhaka Megacity, 219–238.

Dey, N. N., Al Rakib, A., Kafy, A. A., & Raikwar, V. (2021). Geospatial modelling of changes in land use/land cover dynamics using Multi-layer Perceptron Markov chain model in Rajshahi City, Bangladesh. Environmental Challenges, 4, 100148.

Ding, H., & Shi, W. (2013). Land-use/land-cover change and its influence on surface temperature: a case study in Beijing City. International Journal of Remote Sensing, 34(15), 5503–5517.

Imran, H. M., Hossain, A., Islam, A. K. M. S., Rahman, A., Bhuiyan, M. A. E., Paul, S., & Alam, A. (2021). Impact of Land Cover Changes on Land Surface Temperature and Human Thermal Comfort in Dhaka City of Bangladesh. Earth Systems and Environment, 5(3), 667–693.

Kafy, A. A., Faisal, A. A., Hasan, M. M., Sikdar, M. S., Khan, M. H. H., Rahman, M., & Islam, R. (2020a). Impact of LULC Changes on LST in Rajshahi District of Bangladesh: A Remote Sensing Approach. Journal of Geographical Studies.

Kafy, A. A., Rahman, M. S., Faisal, A. A., Hasan, M. M., & Islam, M. (2020b). Modelling future land use land cover changes and their impacts on land surface temperatures in Rajshahi, Bangladesh. Remote Sensing Applications: Society and Environment.

Kanti Jodder, P., Kabir Noyon, E., Bashit, S., & Islam, M. (2020). Proposing Major BRT Routes for Rajshahi City Towards Increasing Public Transport Demand and Alleviation of Congestion Level to Achieve A Sustainable Urban Public Transport System. American Journal of Engineering and Technology Management, 5(4), 61.

NASA. (2010). Landsat 4–7 Thermal Data to be Resampled to 30 Meters.

Ogunjobi, K. O., Adamu, Y., Akinsanola, A. A., & Orimoloye, I. R. (2018). Spatio-temporal analysis of land use dynamics and its potential indications on land surface temperature in Sokoto Metropolis, Nigeria. Royal Society Open Science, 5(12), 180661.

Rahman, S. M., Mamoon, M., Islam, M. S., Hossain, S., Haque, R., & Zubair, A. B. M. (2022). Post-displacement status of climate migrants in Rajshahi City, Bangladesh. Regional Sustainability, 3(3), 183–187.

(Rajshahi Development Authority), RDA. (2008). Working paper on existing landuse, demographic and transport (revised) Government of the People's Republic of Bangladesh Ministry of Housing and Public Works. Rajshahi Development Authority.

Rouf, M. A. (2018). Twentieth Century Urbanization in Bangladesh and a Spell of High and Unsustainable Urban Growth. International Journal of Architecture and Urban Development, 8(3), 5-14.

Tanjina Hasnat, G. (2022). Assessment of spatiotemporal distribution pattern of land surface temperature with incessant urban sprawl over Khulna and Rajshahi City Corporations. Environmental Challenges, 9, 100644.